s, and a recycle time of 0.9 s was used. The spectral widths selected were 16129 Hz (160 ppm) for carbon and ±1410 Hz for proton, with an initial data matrix size of 256 W × 4K (t_1, t_2). The data were processed in the usual fashion. The experiment was performed on approximately 50 mg of pulvomycin, dissolved in 0.5 mL of CD_3OD, and accumulation of data required approximately 14 h.

Acknowledgment. We thank Dr. Tishler (Wesleyan University) and Dr. Stapley (Merck Institute) for making the strain MA-2465 available to us and Mlle Gerardot and Dr. Monteil (Institut de Bacteriologie, Strasbourg) for the strain of *B. subtilis*. We also thank the Science and Engineering Research Council for financial support.

Registry No. 12, 95740-54-8.

The Generation and Trapping of the High-Temperature Cation Radicals $^{28}SiO^+$ and $^{29}SiO^+$ in Neon Matrices at 4 K; An ESR and ab Initio CI Theoretical Investigation

Lon B. Knight, Jr.,*† A. Ligon,† R. W. Woodward,† David Feller,‡ and E. R. Davidson‡

Contribution from the Chemistry Departments, Furman University, Greenville, South Carolina 29613, and the University of Washington, Seattle, Washington 98195.
Received September 17, 1984

Abstract: The high-temperature cation radicals $^{28}SiO^+$ and $^{29}SiO^+$ have been generated by both electron bombardment and photoionization methods and trapped in neon matrices at approximately 4 K for detailed ESR (electron spin resonance) studies. The SiO(g) sample was prepared by the high-temperature (≈2000 K) vaporization of SiO(s) and SiO_2(s). The magnetic parameters obtained for $^{29}SiO^+$ in neon are the following: $g_\parallel = 2.0012$ (2); $g_\perp = 2.0000$ (2). For ^{29}Si $A_\parallel = -924$ (1) MHz and $A_\perp = -733$ (1) MHz. Analysis of the SiO^+(g) tensor clarifies the assignment of an electronic band ($X^2\Sigma \leftarrow B^2\Sigma$) previously associated with both SiO^+ and SiN. Extensive ab initio calculations have been conducted which yield ^{29}Si hfs in good agreement with the experimental results, although redefinition of orbitals used in the CI via MCSCF or INO procedures was required. A population analysis of the valence orbitals for SiO^+, CO^+, AlO, and BO has been made with the results compared to those obtained from the commonly applied procedure for estimating percent "s" or "p" character from "free atom" hyperfine parameters. Significant differences between the two methods were obtained for SiO^+ and AlO. A major deficiency of the free atom comparison method in these two cases was attributed to oxygen valence overlap effects on the core electrons of the metal.

The ESR (electron spin resonance) rare gas matrix isolation technique has been used to investigate several high-temperature (>1000 K) neutral radicals;[1-4] however, no high-temperature cation (or anion) radicals have been studied. Gas-phase ESR measurements of such radicals cannot be conducted by currently available methods. These results for SiO^+ demonstrate the feasibility of combining high-temperature vaporization with the various ion generation and neon matrix trapping techniques developed in recent studies of $^{13}CO^+$,[5,6] $^{15}N_2^+$,[7] $H_2{}^{17}O^+$,[8] $H_2{}^{13}CO^+$,[9] CH_4^+,[10] and Cd^+.[11] Application of the methods to numerous other important inorganic and nonvolatile systems should be straightforward. These techniques have already been adapted for the matrix trapping of ion–neutral reaction products such as $C_2O_2^+$[12] and N_2CO^+[13] and the paramagnetic metal cluster cations Mg_2^+, Mg_3^+, and Mg_6^+.[13] Laser vaporization/ionization methods for trapping cation radicals of refractory materials and matrix codeposition reactions of metal ions with various volatile reagents are currently being investigated by matrix ESR in our laboratory.

The $SiO^+(X^2\Sigma)$ species was selected to be the first high-temperature candidate investigated in detail for the following reasons. Magnetic data comparison with $CO^+(X^2\Sigma)$ can be used to probe electronic and bonding changes that occur as carbon is replaced by silicon in a "simple" diatomic molecule. Detailed comparison of ^{29}Si ($I = {}^1/_2$) nuclear hfs (hyperfine structure) in $^{29}SiO^+$ with previously reported ^{13}C hfs of $^{13}CO^+$ is presented. Experimental conditions for the high-temperature formation of SiO(g) have been established in earlier vibrational (IR) matrix experiments[14,15] which were repeated at the beginning of this study to ascertain that neutral SiO(g) was being generated in reasonable quantities prior to the application of ionization techniques. Magnetic parameters for SiO^+ are particularly interesting since it is isoelectronic to the previously studied high-temperature neutral radical AlO.[16] Electronic structures of these radicals are compared by both theoretical and experimental results. Distinguishing between the electronic bands of SiO^+ and SiN has proven to be a difficult problem.[17,18,19] The **g** tensor measurements obtained in this study

†Furman University.
‡University of Washington.

(1) Weltner, W., Jr. "Magnetic Atoms and Molecules"; Van Nostrand-Reinhold Co., Inc.: New York, 1983.
(2) Kasai, P. H.; Whipple, E. B.; Weltner, W., Jr. *J. Chem. Phys.* **1966**, *44*, 2581.
(3) Knight, L. B., Jr.; Wise, M. B.; Fisher, T. A.; Steadman, J. *J. Chem. Phys.* **1981**, *74*, 6636.
(4) Lindsay, D. M.; Thompson, G. A. *J. Chem. Phys.* **1982**, *77*, 1114. Howard, J. A.; Sutcliffe, R.; Tse, J. S.; Mile, B. *Chem. Phys. Lett.* **1983**, *94*, 561. Baumann, C. A.; Van Zee, R. L.; Bhat, S. V.; Weltner, W., Jr. *J. Chem. Phys.* **1983**, *78*, 190.
(5) Knight, L. B., Jr.; Steadman, J. *J. Chem. Phys.* **1982**, *77*, 1750–1756.
(6) Knight, L. B., Jr.; Steadman, J. *J. Am. Chem. Soc.* **1984**, *106*, 900–902.
(7) Knight, L. B., Jr.; Bostick, J. M.; Woodward, R. W.; Steadman, J. *J. Chem. Phys.* **1983**, *78*, 6415.
(8) Knight, L. B., Jr.; Steadman, J. *J. Chem. Phys.* **1983**, *78*, 5940.
(9) Knight, L. B., Jr.; Steadman, J. *J. Chem. Phys.* **1984**, *80*, 1018–1025.
(10) Knight, L. B., Jr.; Steadman, J.; Feller, D.; Davidson, E. R. *J. Am. Chem. Soc.* **1984**, *106*, 3700.
(11) Knight, L. B., Jr.; Miller, P. K.; Steadman, J. *J. Chem. Phys.* **1984**, *80*, 4587.
(12) Knight, L. B., Jr.; Steadman, J.; Miller, P. K.; Bowman, D. E.; Davidson, E. R.; Feller, D. *J. Chem. Phys.* **1984**, *80*, 4593.
(13) Knight, L. B., Jr.; Steadman, J.; Ligon, A.; Barnett, C. D., to be published.
(14) Anderson, J. S.; Ogden, J. S. *J. Chem. Phys.* **1969**, *51*, 4189.
(15) Hastie, J. W.; Hauge, R. H.; Margrave, J. L. *Inorg. Chim. Acta* **1969**, *3*, 601.
(16) Knight, L. B., Jr.; Weltner, W., Jr. *J. Chem. Phys.* **1971**, *55*, 5066.

0002-7863/85/1507-2857$01.50/0

of SiO^+ clearly support the most recent gas-phase electronic assignments presented by other investigators.[19] The upper atmospheric chemistry of SiO and SiO^+ has been investigated, and significant concentrations of SiO^+ relative to Si^+ have been found in the ionosphere.[20,21] The presence of these species is thought to arise from meteor ablation. Given the presence of SiO in dense interstellar clouds[22] and sun spot activity,[23] SiO^+ is a likely interstellar candidate whose identification might be facilitated by the magnetic parameters reported here.

Apparently no previous ab initio evaluation of one-electron properties has been reported for SiO^+. The theoretical investigation of SiO^+ proved to be most interesting since the RHF/CI and MCSCF wave functions exhibited grossly different ^{29}Si hyperfine structure (hfs). Experimental nuclear hfs clearly showed that HF orbitals were not adequate for describing the electronic structure of SiO^+. A similar occurence was observed in the comparison of theoretical spin densities with experimental hfs results for the isoelectronic AlO radical.[16,24]

An extensive theoretical analysis was conducted for SiO^+ to test the accuracy of a commonly applied approximate procedure for obtaining percent "s" and "p" valence orbital character from the isotropic and dipolar components of the nuclear hfs for a given atom. Ordinarily, such molecular hyperfine parameters are compared directly to analogous parameters for "free" atoms to estimate the percent "s" and "p" valence orbital character in the molecule. A population analysis conducted on a CI wave function which produced A_{iso} and A_{dip} values in good agreement with experiment for ^{29}Si in $^{29}SiO^+$ yielded valence "s" and "p" percentages that were significantly different from those obtained by the free atom comparison method (FACM). For example, the FACM indicates a valence s/p_σ ratio of 0.30 compared to a value of 1.1 obtained from the population analysis procedure. The findings of this in-depth treatment should help identify similar electronic structures in other radicals that are particularly unsuitable for FACM. Other limitations of FACM have been discussed previously.[1]

Experimental Section

Details of the matrix apparatus, ESR spectrometer, and computer system have been presented in previous reports.[5,7,9] The open tube neon discharge source (17 eV) described in the CO^+ study[5] was used to photoionize SiO(g) produced from vaporized samples of SiO(s) and SiO_2(s). Photoionization of SiO(g) was conducted during neon matrix deposition. Neon matrix samples of SiO^+ were also formed from SiO(g) by the recently developed electron bombardment matrix procedure.[7] This independent generation method produced ESR spectra of SiO^+ identical with those obtained with photoionization. The identities of possible counteranions also trapped during these matrix experiments have been discussed previously.[5-8] The most likely candidates are not radicals and hence not detectable by ESR.

Vaporization of the silicon oxide samples was conducted in standard resistively heated Knudsen cells constructed entirely of tantalum. The vaporization oven assembly (tantalum tube with end caps and strap supports) was mounted on water-cooled copper electrodes. The 1.5-mm effusion orifice in the vaporization cell was 10 cm from the copper matrix deposition target (4 cm × 0.6 cm × 0.15 cm). The deposition target was cooled to ≈5 K by a modified Air Products Heli-Tran cryostat mounted on hydraulic lifters for transporting the target 5 cm between the deposition position and the ESR cavity mounted inside the vacuum system. The neon (Matheson research grade) flow rate was 18 mmol h^{-1} for the standard deposit of 1 h. Typical background pressures in the apparatus after outgassing the cell and sample were 4.7×10^{-7} torr. During deposition and with the open tube neon discharge lamp operating, the pressure in the vicinity of the target rose to $\approx 8 \times 10^{-5}$ torr. The amount of neon gas entering the system from the discharge lamp was approximately 5% of the total neon directed toward the deposition surface. The microwave discharge power level employed was 60 W with a reflected power of 2 W. As observed for other molecular cations having electron affinities greater than 11–12 eV, similar experiments in argon matrices failed to produce ESR signals attributable to charged radicals.[5,7,8,25] This presumably results from the considerably higher ionization energy of neon vs. argon.

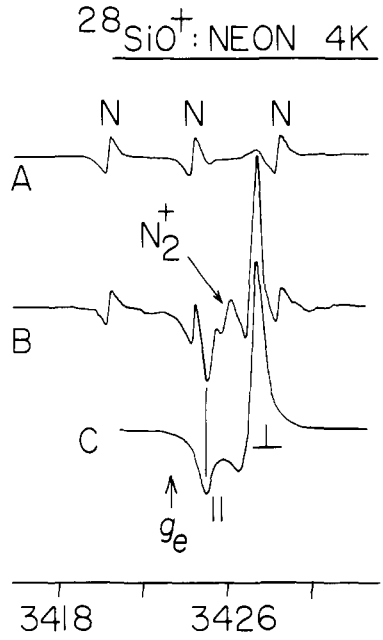

Figure 1. High-temperature deposition of ^{28}SiO(g) into a neon matrix during photoionization at 17 eV produced the ESR spectrum shown in B. The parallel and perpendicular type lines are assigned to the $^{28}SiO^+$ ($X^2\Sigma$) radical. Other features in B result from the ^{14}N (I = 1) triplet and the central line of the $^{14}N_2^+$ quintet. Visible photolysis or bleaching of B produced the A spectrum, which shows virtual elimination of the $^{14}N_2^+$ line and the $^{28}SiO^+$ features (see text). Spectrum C is a computer-simulated powder pattern having the SiO^+ $g_\parallel$ and $g_\perp$ values listed in Table I. The magnetic field position for the free electron is denoted by g_e.

In a series of separate deposition experiments, SiO(s) and SiO_2(s) powders (Alfa Products Puratronic 99.999%) containing natural abundance silicon (^{29}Si, 4.7%) were vaporized over the temperature ranges 1150–1650 and 1600–1900 K, respectively. Consistent with the original vibrational matrix studies of SiO, the strongest $^{28}SiO^+$ ESR signals were observed at the highest vaporization temperatures for these two ranges. A $^{29}SiO_2$(s) sample containing 88% enrichment in ^{29}Si was obtained from Oak Ridge Laboratories and vaporized in a similar manner. However, it was observed that higher temperatures were required to yield intense $^{29}SiO^+$ ESR signals. This higher temperature requirement probably resulted from the partial filling of the Knudsen cell with the expensive isotopic sample and the lower ESR sensitivity for a radical with anisotropic nuclear hyperfine structure (hfs). A total of 37 separate high-temperature matrix deposition experiments were conducted during the course of these studies to optimize the generation of SiO^+ from ^{Nat}SiO(s), $^{Nat}SiO_2$(s), and $^{29}SiO_2$(s) by both photoionization and electron bombardment methods.

Results

$^{28}SiO^+$. Figure 1B presents an expanded scale ESR spectrum centered near g_e which exhibits nitrogen atom impurity lines, the symmetric central line ($M_J = 0$) of the previously characterized $^{14}N_2^+$ quintet,[7] and a highly anisotropic powder pattern. The powder pattern consisting of a weak parallel and a strong perpendicular feature was observed only when a silicon oxide sample was vaporized and matrix isolated under ionizing conditions. These signals were considerably more intense when ^{Nat}SiO and $^{Nat}SiO_2$ (^{28}Si natural abundance ≈ 95%) samples were vaporized compared to isotopically enriched $^{29}SiO_2$ which contained only 12% ^{28}Si. The

(17) Nagaraj, S.; Verma, R. D. *Can. J. Phys.* **1968**, *46*, 1597.
(18) Dunn, T. M.; Rao, K. M.; Nagaraj, S.; Verma, R. D. *Can. J. Phys.* **1969**, *47*, 2128.
(19) Singh, M.; Bredohl, H.; Remy, F.; Dubois, I. *J. Phys. B*: **1973**, *6*, 2656.
(20) Ferguson, E. E.; Fehsenfeld, F. C.; Whitehead, J. D. *J. Geophys. Res., A* **1970**, *75*, 4366.
(21) Fehsenfeld, F. C. *Can. J. Chem.* **1969**, *47*, 1808.
(22) Wolff, Richard S. *Astrophys. J.* **1980**, *242*, 1005.
(23) Joshi, G. C.; Punetha, L. M.; Pande, M. C. *Sol. Phys.* **1979**, *62*, 77.
(24) Knight, L. B., Jr.; Wise, M. B.; Davidson, E. R.; McMurchie, L. E. *J. Chem. Phys.* **1982**, *76*, 126.
(25) Andrews, L.; Keelan, B. W. *J. Am. Chem. Soc.* **1980**, *102*, 5732. Bondybey, V. E.; English, J. H.; Miller, T. A. *J. Chem. Phys.* **1979**, *70*, 1621.

Table I. Magnetic and Electronic Structure Comparisons of SiO^+ with CO^+ and the Isoelectronic $^2\Sigma$ Neutral Radical AlO

	$g_\parallel$	$g_\perp$	$A_\parallel$[a]	$A_\perp$[a]	A_{iso}[a]	A_{dip}[a]	% "s"[b]	% "p"[b]
$^{29}Si^{16}O^+$[c]	2.0012 (2)	2.0000 (2)	−924 (1)	−733 (1)	−797 (1)	−64 (1)	17	56
$^{28}SiO^+$[c]	2.0013 (2)	2.0000 (2)						
CO^+: ^{13}C[d]	2.0004 (7)	1.9996 (5)	1665 (2)	1527 (2)	1573 (2)	46 (1)	42	43
CO^+: ^{17}O[e]	2.0011 (4)	1.9995 (2)	−47.6 (9)	51.5 (6)	18.5 (5)	−33.0 (5)	−0.35	20
$^{27}Al^{16}O$[f]	2.0015 (3)	2.0004 (3)	872 (1)	713 (1)	766 (1)	53 (1)	20	64

[a] The signs of the hyperfine components given in MHz are taken as the sign of the respective nuclear magnetic moments since absolute signs cannot be determined by the measurements. However, positive spin density seems most reasonable for all entries except for $A_{iso}(^{17}O)$ in $^{12}C^{17}O^+$. [b] Percent "s" and "p" character for the unpaired electron was determined by comparing molecular values of A_{iso} and A_{dip} with analogous atomic values listed by Morton and Preston in ref 26. The values obtained by this free atom comparison method (FACM) for SiO^+ and AlO differ significantly from a detailed population analysis of a CI wave function. See text and Tables IV and V. [c] Neon matrix, current study. [d] Neon matrix, ref 5. [e] Neon matrix, ref 6. [f] Neon matrix, ref 16.

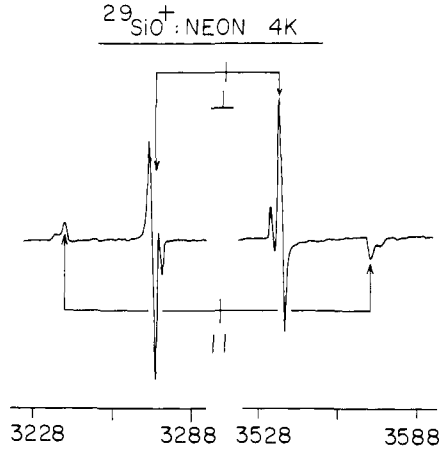

Figure 2. Neon matrix ESR spectrum of $^{29}SiO^+$ exhibiting ^{29}Si ($I = {}^1/_2$) parallel and perpendicular hyperfine lines is shown. The nonlabeled less-intense features are assigned to $^{29}SiO^+$ in an alternate trapping site in the neon lattice (see text). The magnetic field corresponding to g_e is 3406.8 (1).

N atom and $^{14}N_2^+$ lines are usually observed on blank depositions without silicon oxide vaporization.

The spectrum in Figure 1A was recorded after visible photolysis of the matrix sample shown in Figure 1B. Note that the powder pattern and the $^{14}N_2^+$ line are virtually absent in Figure 1A. Visible photolysis of the matrix sample has been shown to be a very useful diagnostic tool in identifying ESR lines associated with charged radicals. The low-energy (2–3 eV) visible photons can presumably photoionize the electron traps or counteranions (A^-), producing mobile electrons which can react with cation radicals throughout the neon lattice. Figure 1C presents a computer simulated spectrum of a powder pattern having $g_\parallel$ and $g_\perp$ values assigned to the analogous features in Figure 1B. The g values for $^{28}SiO^+$ are listed in Table I.

The observed ESR features of Figure 1B are the expected ones for a randomly oriented sample of axially symmetric $^{28}SiO^+(X^2\Sigma)$ with no ^{28}Si ($I = 0$) or ^{16}O ($I = 0$) nuclear hfs. As discussed in a latter section the observed value of $\Delta g_\perp$ ($\Delta g_\perp = g_\perp - g_e$) is consistent with gas-phase spectroscopic measurements of the spin-doubling parameter.

$^{29}SiO^+$. Confirmation of the above $^{28}SiO^+$ ESR assignment was obtained from an analysis of the ^{29}Si ($I = {}^1/_2$; $\mu = -0.5553$) hfs in the $^{29}SiO^+$ ESR spectrum shown in Figure 2. The **g** and **A** tensor parameters for $^{29}SiO^+$ listed in Table I were determined from the indicated parallel and perpendicular line positions with the standard second-order resonance field expressions for the axially symmetric case[1]

$$H_\parallel = H_\parallel^\circ - M_I A_\parallel - \frac{A_\perp^2}{2H_\parallel^\circ}[I(I+1) - M_I^2]$$

$$H_\perp = H_\perp^\circ - M_I A_\perp - \frac{(A_\parallel^2 + A_\perp^2)}{4H_\perp^\circ}[I(I+1) - M_I^2]$$

where $H_\parallel^\circ = h\nu/g_\parallel\beta$ and $H_\perp^\circ = h\nu/g_\perp\beta$. This analysis for $^{29}SiO^+$ yields $g_\parallel$ and $g_\perp$ values identical with those observed for $^{28}SiO^+$ within the experimental uncertainty of ±0.2 G. For a spectrometer frequency of $\nu = 9547.4$ (3) MHz, the $^{28}SiO^+$ parallel and perpendicular lines were observed at 3408.6 (2) and 3410.7 (1) G, respectively. For $^{29}SiO^+$, the parallel lines occurred at 3238.9 (3) and 3568.9 (3) G and the perpendicular features at 3273.1 (2) and 3535.1 (2) G.

The observed powder pattern line shapes and relative phases of the low- and high-field $^{29}SiO^+$ lines follow expected behavior and are similar to the $^{13}CO^+$ spectrum except for the smaller magnitude of the ^{29}Si **A** values. The $^{29}SiO^+$ ESR lines demonstrated the same rate of decrease with visible photolysis as the $^{28}SiO^+$ lines in the g_e area and practically the same intensity response with changes in the incident microwave power which was varied over the range of 3 mW to 1 μW. The extra lines in Figure 2 most probably result from multiple trapping sites in the neon lattice which produce ≈2% differences in the large ^{29}Si hfs. The relative intensity of these weaker sites varied considerably among the different depositions, and these sites were preferentially destroyed by repeating annealing cycles. An annealing cycle consisted of warming the neon matrix from ≈5 to 9 K for several minutes before rapid quenching to 5 K.

Consistent with previous attempts to trap other small cation radicals in argon matrices,[5] no ESR signals were detected in argon which could be associated with $^{28,29}SiO^+$ radicals. Weak ESR signals were detected at similar magnetic field positions in both neon and argon matrices that apparently exhibited large ^{29}Si hfs. These unidentified lines were not affected by prolonged visible photolysis and hence most probably do not belong to charged radical species. The assignment of these neutral silicon-containing radicals will require additional experiments which are currently in progress. A careful search for $Si_2O_2^+$ and $Si_3O_3^+$ radicals was made since such polymeric neutrals have been detected in IR matrix studies[14,15] and $C_2O_2^+$ has been fully characterized in a recent ESR investigation.[12] However, no ESR patterns were detected which could be associated with such silicon oxide polymeric cation radicals. It is possible that these larger silicon species are dissociated by the ionizing conditions present during matrix deposition.

Discussion

^{29}Si hfs. The values of $A_\parallel$ and $A_\perp$ for $^{29}SiO^+$ listed in Table I are related to the A_{iso} and A_{dip} parameters by the following simple equations since $g_\perp$ shows little deviation from g_e

$$A_{iso} = {}^1/_3(A_\parallel + 2A_\perp)$$

$$A_{dip} = {}^1/_3(A_\parallel - A_\perp)$$

$$A_{iso} = {}^8/_3\pi g_e g_n \beta_e \beta_n \langle\delta(r)\rangle$$

$$A_{dip} = {}^1/_2 g_e g_n \beta_e \beta_n \left\langle \frac{3\cos^2\theta - 1}{r^3} \right\rangle$$

where all symbols have their standard definitions and the average is over the spin density. The results of a detailed ab initio CI calculation of A_{iso} and A_{dip} for $^{29}SiO^+$ are presented in a subsequent section.

In Table I the values of A_{iso} and A_{dip} for $^{29}SiO^+$ are compared with similar quantities for $^{13}C^{16}O^+$, $^{12}C^{17}O^+$, and the isoelectronic

$^2\Sigma$ neutral radical AlO. Conversion of the A_{iso} and A_{dip} values into percent "s" and "p" character for "the orbital containing the unpaired electron" is generally believed to be useful in making electronic structure comparisons among similar radicals. These % "s" and % "p" results based on Morton and Preston's[26] set of atomic A_{iso} and A_{dip} parameters are also listed in the last two columns of Table I. FACM (free atom comparison method) analysis indicates that the total spin density on C (85%) in CO^+ remains similar to that of Si (73%) in SiO^+ while the s/p hybridization ratio decreases dramatically from $\approx$1 in CO^+ to $\approx$0.30 in SiO^+. The 84% total spin density on Al in AlO shows an s/p ratio of $\approx$0.31 which is practically indistinguishable from the value for isoelectronic SiO^+. Comparison of spin densities and s/p ratios has recently been discussed for the analogous first-row 13-electron $^2\Sigma$ diatomic radicals $^{15}N_2^+$, $^{13}C^{14}N$, $^{13}C^{17}O^+$, $^{11}B^{17}O$, and $^9Be^{19}F$.[6] As will be shown in a later section, the populations derived in this way for second-row elements are in serious disagreement with analysis of actual wave functions. Further, these FACM results for CO^+ and SiO^+ differ from the expected trend of less, rather than more, s/p hybridization in the second row compared to the first row.

g Tensor. The observed neon matrix value of $\Delta g_\perp$ ($\Delta g_\perp = g_\perp - g_e$) for SiO^+ listed in Table I is consistent with the most recent electronic spectroscopic measurement of the ground-state spin-rotational coupling constant γ.[19] This is important since other electronic studies[18] conducted since Woods'[27] original work had reassigned the $SiO^+(X^2\Sigma \leftarrow B^2\Sigma)$ band system at $\approx$26 000 cm^{-1} to the isoelectronic neutral radical, SiN. SiN does have a similar transition at $\approx$24 000 cm^{-1}, but its γ parameter[28] is large and negative (−0.0173 cm^{-1}) relative to that for SiO^+[19] which is small and positive (+0.0028 cm^{-1}). The Curl equation[29] gives the following simple relationship between γ and $\Delta g_\perp$ and can therefore be used as an independent check on the difficult electronic assignment problem for SiO^+ and SiN

$$\gamma = -2B\Delta g_\perp$$

where B is taken to be the ground-state rotational constant. This relationship has been previously applied to numerous diatomic neutral radicals and has been shown to be accurate within approximately 10%.[30] The Curl equation predicts a $\Delta g_\perp$ of −0.0019 based on the most recent SiO^+ electronic measurement of γ. This result compares favorably with the $\Delta g_\perp$ value of −0.0023 (2) listed in Table I for these neon matrix ESR results for SiO^+. The SiN γ value would predict a $\Delta g_\perp$ of +0.0118 which is well outside the ESR experimental uncertainty limits. Hence, a clear **g** tensor distinction between these "similar" radicals can be made. Experimental efforts are currently in progress to generate and trap SiN for detailed study.

The small value of $\Delta g_\perp$ for SiO^+ is particularly interesting, and a qualitative explanation for this occurence involving spin–orbit coupling with both an excited $^2\pi_r$ and $^2\pi_i$ state is proposed. This explanation is also consistent with the experimental observation that $\Delta g_\perp$ for CO^+ is practically the same as that for SiO^+ even though the atomic spin–orbit parameter for Si is nearly five times that of a C atom. Unfortunately, the excited $^2\pi$ states of SiO^+ have not been located spectroscopically. The isoelectronic neutral AlO radical has a low-lying $^2\pi_i(...\sigma^2\pi^3\sigma^2)$ state at 5400 cm^{-1} and a $^2\pi_r(\sigma^2\pi^4\pi^1)$ state at 33 000 cm^{-1}.[16] Assuming the existence of similar states for SiO^+, the unpaired electron in the $^2\pi_i$ state should have large O $2p_\pi$ character while the $^2\pi_r$ state would likely have predominantly Si $3p_\pi$ character. Spin–orbit coupling to both excited $^2\pi$ states would be important if the ground $^2\Sigma$ state had significant p_σ contributions from both Si and O. Neglecting overlap and higher order effects, spin–orbit coupling to $^2\pi_r$ states reduces $g_\perp$ relative to g_e and coupling to $^2\pi_i$ states increases $g_\perp$.[1]

Table II. Orbital Occupancy of the Reference Configurations for SiO^+

	σ			π_x			π_y		
	6	7	8	1	2	3	1	2	3
(1)	2	1		2	2		2	2	
(2)	2	1		2	1	1	2	1	1
(3)	2	1		2		2	2	2	
(4)	2	1		2	2		2		2
(5)	1	2		2	2		2	2	
(6)	1	2		2	2		2	1	1
(7)	1	2		2	1	1	2	2	
(8)	1	1	1	2	2		2	2	
(9)	2	1		2		2	2		2
(10)	2	1		2	2		2	1	1
(11)	2	1		2	1	1	2	2	
(12)	2	1		2		2	2	1	1
(13)	2	1		2	1	1	2		2
(14)	1	2		2	2		2		2
(15)	1	2		2		2	2	2	
(16)	1	2		2		2	2		2
(17)	1	2		2	1	1	2	1	1
(18)	1	2		2		2	2	1	1
(19)	1	2		2	1	1	2		2

The large increase in O p_σ character (0.41) in SiO^+ relative to CO^+ (0.06) (based on the Mulliken population analysis of Table IV) would result in greater spin–orbit coupling to the excited $^2\pi_i$ state and hence partially cancel the increased coupling to the $^2\pi_r$ state that should result from the larger spin–orbit parameter of Si (ξ = 146 cm^{-1}) relative to C (ξ = 28 cm^{-1}).

Theoretical Calculations for SiO^+. The isoelectronic radical AlO has the same $^2\Sigma$ ground-state electronic configuration as SiO^+: $(X^2\Sigma^+)\ 1\sigma^2 2\sigma^2 3\sigma^2 4\sigma^2 5\sigma^2 6\sigma^2 7\sigma^1 1\pi^4 2\pi^4$. While no ab initio calculations of one-electron properties have been previously reported for SiO^+, experimental and theoretical spin-density results have been compared for AlO.[24] In that work the existence of two distinct solutions to the restricted Hartree–Fock (RHF) equations necessitated the use of an iterative natural orbital[31] (INO) approach to defining the orbitals. One of the two SCF wave functions had the singly occupied 7σ orbital localized on the oxygen atom, while the highest doubly occupied orbital was more covalent in nature. In the other solution the nature of the 6σ and 7σ orbitals was reversed. The Hartree–Fock one-electron properties, including the hyperfine splitting parameters, were strongly dependent on which of these two wave functions was used.

The AlO INO configuration interaction (CI) wave functions involved all single excitations from 18 of the space orbital products listed in Table II (1–7 and 9–19). This list was obtained by coupling the $...6\sigma^2 7\sigma^1$ and $...6\sigma^1 7\sigma^2$ σ occupancies with all possible arrangements of the four π electrons among the ($2\pi_x$, $3\pi_x$, $2\pi_y$, $3\pi_y$) orbitals. A Dunning–Hay[32,33] [6s,4p,2d/4s,2p,1d] contracted basis set was used in the AlO calculations. In this notation the metal portion of the basis is given in front of the slash mark, and the oxygen portion is given after it. Following convergence of the INO one-electron properties, the final AlO CI hyperfine coupling constants were in good agreement with the available experimental data.

Ab initio calculations have also been performed on CO^+ ($^2\Sigma^+$),[12] the second-period analogue of SiO^+, and on BO, the analogue of AlO.[24] No apparent complications arose from multiple SCF solutions, and agreement between the final CI properties and the available matrix and gas-phase values was within several percent. In these radicals the odd electron is almost entirely on the carbon or boron atom, as judged by a total spin density greater than 95%.

All SiO^+ calculations in the present study were carried out at the fixed experimental equilibrium bond length of 1.504 Å.[34] Two

(26) Morton, J. R.; Preston, K. F. *J. Magn. Reson.* **1978**, *30*, 577.
(27) Woods, L. H. *Phys. Rev.* **1943**, *63*, 426.
(28) Bredohl, H.; Dubois, I.; Houbrechts, H.; Singh, M. *Can. J. Phys.* **1976**, *54*, 680.
(29) Curl, R. F. *Mol. Phys.* **1965**, *9*, 585.
(30) Knight, L. B., Jr.; Weltner, W., Jr. *J. Chem. Phys.* **1970**, *53*, 4111. See also pp 50–52 of ref 1.
(31) Bender, C. F.; Davidson, E. R. *J. Phys. Chem.* **1966**, *70*, 2675.
(32) Dunning, T. H., Jr. *J. Chem. Phys.* **1970**, *53*, 2823.
(33) Dunning, T. H., Jr.; Hay, P. J. "Methods of Electronic Structure Theory"; Schaefer, H. F., III, Ed.; Plenum: New York, 1977: p 23.
(34) Huber, K. P.; Herzberg, G. "Molecular Spectra and Molecular Structure"; Van Nostrand-Reinhold Co., Inc.: New York, 1979.

Table III. Theoretical Results for $^{29}SiO^+(^2\Sigma^+)$[a]

basis set	wave function	% Si	A_{iso} (^{29}Si)	% O	A_{iso} (^{17}O)
DZP[b]	RHF, E = −363.4119	15	−26	84	−167
	all singles CI, E = −363.4321; 564 spin-adapted config		132		−98
	MCSCF, E = −363.4966; 35 spin-adapted config	51	−745	47	−43
	NO-CI (cycle 1), E = −363.5650; all singles from 35 config	59	−810	40	3
	NO-CI (cycle 2), E = −363.5631	60	−849	39	10
	NO-CI (cycle 3), E = −363.5620	60	−861	39	10
	MR-NO-SD-CI, E = −363.7174; 15 831 config selected from 1 233 613 generated; 36 ref config	56	−746	42	8
	MR-NO-SD-CI, E = −363.7275; 15 840 config selected from 602 089 generated; 14 ref config	57	−758	41	11
extended[c]	RHF, E = −363.4506	16	−24	83	−160
	all singles CI, E = −363.4711; 647 spin-adapted config		133		−100
	MR-NO-SD-CI, E = −363.9036; 21 258 config selected from 2 926 804 generated; 14 ref config	55	−757	42	12

[a] Energies are in hartrees, isotropic hyperfine parameters are given in MHz. The following conversion factors were used for converting $8\pi/3\langle\delta(r)\rangle$ in atomic units to A_{iso}, MHz: −106.1 (^{29}Si), −72.4 (^{17}O). These were obtained by multiplying 95.53 MHz/au by the appropriate nuclear g value (^{29}Si = −1.1106 and ^{17}O = −0.7575). % Si and % O refer to the percent of the spin density attributed to Si and O by a Mulliken population analysis. [b] The Dunning–Hay (11s,7p,2d/9s,5p,1d) to [6s,4p,2d/4s,2p,1d] contraction. [c] An (18s,12p,3d/12s,6p,2d) to [12s,8p,3d/8s,4p,2d] contraction.

basis sets were used. Preliminary phases of this investigation employed an (11s,7p,2d/9s,5p,1d) primitive set contracted to [6s,4p,2d/4s,2p,1d]. The oxygen portion of this basis had been used previously in work on a variety of small radicals.[35] We shall subsequently refer to this basis as the double-ζ polarization (DZP) basis. Exponents for the two d polarization functions on silicon (0.15 and 0.45) were taken from the work of Wood and Hillier.[36] A standard d exponent of 0.85 was used on oxygen.

The second set, which we shall refer to as the "extended" basis, consisted of an (18s,12p,3d/12s,6p,2d) even-tempered[37] set of primitives contracted to [12s,8p,3d/8s,4p,2d]. Polarization exponents (0.23, 0.67, and 2.90 on Si, 0.70 and 1.86 on O) were obtained by partially optimizing their values in SCF calculations on SiO^+. This set produced an SCF energy for the neutral molecule of −363.8458 hartrees compared to the near-Hartree–Fock value of McLean and Yoshimine[38] of −363.8523 hartrees. The SiO^+ bond length, which is only 0.006 Å shorter than the neutral, was used.

Both of these basis sets have several s orbitals in the 1s core but no higher angular momentum functions of that size. As a consequence, they should be able to describe the core contribution to the contact interaction fairly well, but they will not give an accurate estimate of any core contribution to the anisotropic hyperfine. Previous calculations[24] on BO showed such core anisotropic effects to be small.

Table III lists the energies and properties resulting from a variety of theoretical treatments. The first thing which will be noticed is the very small isotropic hyperfine, $A_{iso}(^{29}Si)$, value obtained at the SCF level. This is due to the odd-electron localization on oxygen, as already mentioned. This localization is obvious in a contour plot of the singly occupied 7σ molecular orbital presented in Figure 3 along with the corresponding orbital in CO^+. Contrary to the case of AlO, no second SCF solution could be found in spite of several attempts to do so. Initial guess orbitals which placed the odd electron on silicon would, after many iterations, converge to the previously found minimum.

Along with unrestricted HF (UHF), one of the most commonly used and computationally fast methods for obtaining ab initio hyperfine properties involves CI with all single excitations from the HF configuration.[39] However, in a case where the SCF wave function is qualitatively wrong, as it is here, the single CI value of $A_{iso}(^{29}Si)$ can modify the SCF value in the wrong direction. Thus, Table III shows all singles CI values of $A_{iso}(^{29}Si)$ with both basis sets to be large and positive.

In light of the experiences with AlO it was evident that some sort of post HF redefinition of the orbitals would be necessary. Originally it was hoped that singles from a subset of the 18 space orbital products previously used for AlO would be sufficient for purposes of orbital relaxation. Thus, INO based on the multireference singles and doubles CI (MR-SD-CI) approach was initially attempted. Using results of preliminary CI's all single and double excitations from space oribtal products 1–8 of Table II were generated.

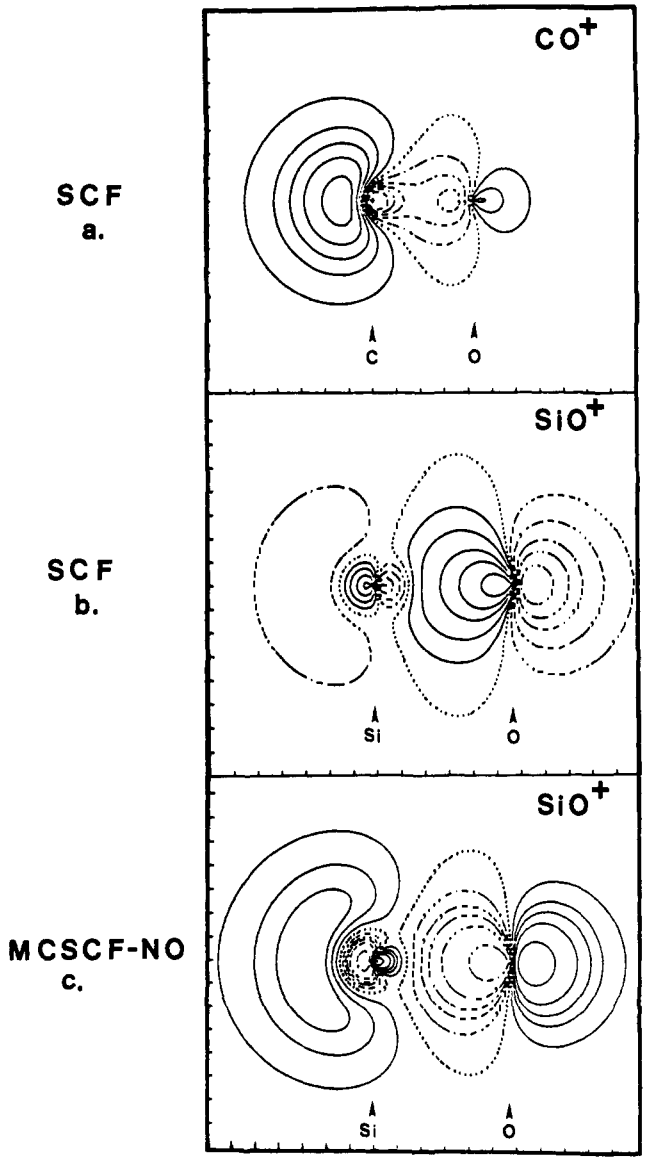

Figure 3. Density contour plot of the singly occupied orbital is shown for (a) CO^+ at the SCF level, (b) SiO^+ at the SCF level, and (c) SiO^+ at the MCSCF NO level. The contours enclose 90, 70, 50, 30, and 10% of the probability density.

(35) Feller, D.; Davidson, E. R. *J. Chem. Phys.* **1984**, *80*, 1006.
(36) Wood, C.; Hillier, I. H. *Mol. Phys.* **1979**, *37*, 1329.
(37) Schmidt, M. W.; Ruedenberg, K. *J. Chem. Phys.* **1979**, *71*, 3951.
(38) McLean, A. D.; Yoshimine, M. *IBM J. Res. Dev. 11*, supplement.
(39) Chipman, D. M. *J. Chem. Phys.* **1979**, *71*, 761.

Although we could afford to variationally treat the relatively small number of single excitations, our inability to handle the millions of doubles required that a selection of these be made on the basis of each configuration's energy contribution to the CI wave function as estimated by second-order perturbation theory. In spite of the fact that a configuration's energy contribution is not necessarily indicative of its importance to a given property, past tests have demonstrated that energy selected MR-SD-CI's can accurately reproduce the properties of nonselected CI's if the zeroth-order wave function is of high enough quality and a sufficiently large fraction of the correlation energy is variationally recovered. One measure of the quality of the reference space is the sum of the squares of the coefficients of the reference configurations in the final CI. In general, numbers on the order of 0.90–0.92 have been shown to be adequate for obtaining reasonable energies and properties. For these calculations, values in the 0.94–0.95 range were obtained. Approximately 86% of the total SD correlation energy was recovered. Both measures would imply a fairly high quality wave function.

However, contrary to the impression created by these indicators, after three INO iterations the $A_{iso}(^{29}Si)$ value of −361 MHz was still only 45% of the experimental value. Furthermore, the INO's had appeared to converge since the NO's generated from the third CI had coefficients on the order of 0.999 in terms of the previous NO's. The CI coefficient of the next largest configuration not included in the reference space was only 0.017.

Due to the poor agreement with experiment several other approaches were attempted with the DZP basis. A multiconfiguration SCF (MCSCF) wave function, in which the CI expansion coefficients and orbital coefficients are simultaneously optimized, produced a much less localized 7σ orbital, shown in Figure 3 along with the original SCF orbital. The A_{iso} value of −745 MHz is much closer to experiment than the −361 MHz of the 8 reference configuration INO CI. This calculation was performed with GAMESS[40] and allowed all excitations of 7 electrons among 6 orbitals (6σ, 7σ, $2\pi_x$, $3\pi_x$, $2\pi_y$, and $3\pi_y$) consistent with the $^2\Sigma$ overall symmetry. Inclusion of the π orbitals in this calculation was necessary because an MCSCF calculation with 3 electrons in (6σ, 7σ) would have merely given the RHF result again. Inclusion of the π orbitals allowed the π bonds to have different polarity when the unpaired electron was on Si than when it was on O.

Unfortunately, an MCSCF calculation with the 86 basis functions of the extended basis is beyond the capabilities of the programs at our disposal. The INO technique used in the AlO study should produce qualitatively the same results as the MCSCF procedure. That this, in fact, is the case can be seen in Table III. The third INO iteration produced an A_{iso} value of −860 MHz which is within 15% of the MCSCF value. Somewhat surprisingly the 8 space orbital products which were used as the reference space in the earlier INO calculations, which yielded A_{iso} = −361 MHz, were still dominant. Thus, it would seem that the combined effect of the single excitations from the 11 minor space orbital products not included in the first INO CI's is required to produce a set of orbitals in qualitative accord with the MCSCF orbitals and experiment.

The effect of the energetically important double excitations on the properties was investigated by extending the CI configuration space to include all singles and doubles from all 19 space orbital products (36 spin-adapted configurations) listed in Table II. As can be seen from the second to last entry under the DZP basis set heading in Table III, the selected doubles slightly improved agreement with experiment. An estimated 91% of the total singles and doubles correlation energy was variationally recovered by the selected configurations. The theoretical silicon isotropic value of −746 MHz is now within 7% of experiment.

However, the corresponding 19 reference space orbital products MR-SD-CI would have generated over 7 million spin-adapted configurations with the extended basis and would have been prohibitively expensive even to scan for the dominant configurations. Thus, it was of interest to see if, once the orbitals had been refined, a subset of the 19 space orbital products would make an adequate zeroth-order reference space. The 8 most important space orbital products (14 spin-adapted configurations) were selected, as judged by the size of their coefficients in the previous MR-NO-SD-CI. These 8 are the same as those used in the very first set of calculations. The isotropic hyperfine parameters with this reference space are listed in the final DZP entry of Table III. They are almost identical with the larger reference space calculations. The calculated hyperfine dipolar term in the direction of the bond is −66 MHz which is only a 3% difference from the experimental value.

The extended basis set MR-SD-CI isotropic results in Table III show no significant improvement over the DZP results. However, due to the increase in the number of configurations (to almost 3 million) it was variationally possible to recover only 81% of the total SD correlation energy. This is somewhat less than the over 90% obtained with the smaller basis. A run with the comparable percentage and the smaller DZP basis gave $A_{iso}(^{29}Si)$ = −734 MHz. This suggests that the extended basis set results may be about 3% smaller in absolute magnitude than the full MR-SD-CI value. If the extended basis set A_{iso} value is multiplied by 1.02 to account for the fact that this basis set gives a value of the MF density at the nucleus which is 2% lower than the HF limit, we obtain a final theoretical estimate of A_{iso} = −771 MHz. The hyperfine dipolar value along the internuclear axis is −69 MHz.

As if to emphasize the widely acknowledged belief that wave functions which produce low energies should not automatically be expected to yield good properties, the energy of the extended basis set INO-CI is almost 0.3 hartree above the energy of the best CI without INO. Although not shown in Table III, a MR-SD-CI calculation with the original SCF occupied/K orbital[41] virtual set had a variational energy within 2 mhartrees of the final CI in that table but predicted A_{Si} to be −202 MHz. Similarly, the extrapolated full CI energy from these two calculations was within several millihartrees of each other. This extrapolation was performed with the expression[42]

$$\Delta E(\text{full CI}) = \Delta E(\text{CI})[1 + E(\text{disc})/E(\text{kept})]c_0/(2c_0 - 1)$$

where ΔE(CI) is the energy lowering from the variational CI calculation and E(disc) and K(kept) are the second-order perturbation theory estimate of the energy corresponding to the configurations which were discarded and kept, respectively. The value of c_0 is taken as the sum of the squares of the reference configurations in the final CI wave function. While the spin properties were not similarly extrapolated in this study, such a procedure may prove to be useful in estimating the effects of the configurations which were not treated variationally.

Spin Population Analysis. Spin properties for BO, CO^+, AlO, and SiO^+ obtained with similar quality DZP basis sets and roughly similar kinds of CI are listed in Table IV. These are not the best theoretical numbers possible, but they are qualitatively similar to the experimental values and they are adequate for examining the difficulties in interpreting the "experimental" spin densities given in Table I obtained by the commonly employed free atom comparison method (FACM). Also included in Table IV are spin populations obtained by two methods. In the first method, the CI spin density matrix was projected onto a minimum set of atomic orbitals and then the Mulliken gross population was computed.[43] The core atomic orbitals for this analysis were chosen to be atomic Hartree–Fock orbitals computed with the same atomic basis set. The valence atomic orbitals were chosen orthogonal to the core in such a way that the singly occupied natural orbital in the leading configuration could be expressed exactly as a linear combination of atomic core and valence orbitals. The CI spin density projected

(40) Dupuis, M.; Spangler, D.; Wendoloski, J. J. NRCC Software Catalog 1980, p 1, Program GG01 (GAMESS).

(41) Feller, D.; Davidson, E. R. *J. Chem. Phys.* **1981**, *84*, 3977.
(42) Davidson, E. R.; Silver, D. *Chem. Phys. Lett.* **1977**, *52*, 403.
(43) Mulliken, R. S. *J. Chem. Phys.* **1955**, *23*, 1833. Davidson, E. R. *J. Chem. Phys.* **1967**, *46*, 3319.

Table IV. Spin Properties and Populations for $^2\Sigma^+$ Diatomics[a]

	BO		CO^+		AlO		SiO^+	
	B	O	C	O	Al	O	Si	O
				Spin Property				
$\langle\delta(r)\rangle$	0.71	0.04	1.38	0.00	0.61	−0.01	0.73	0.03
$\langle 3z^2 - r^2/r^5\rangle$	0.31	0.41	0.76	0.72	0.74	1.38	1.24	1.90
				Mulliken Gross Population				
% s	57	0	51	0	41	0	30	0
% p_z	39	3	41	6	26	31	27	41
% p_x	4	−3	5	−4	2	−2	1	0
% p_y	4	−3	5	−4	2	−2	1	0
total	103	−3	103	−3	73	27	59	41
				Apparent Experimental Population				
% s	40	0	41	0	18	0	14	0
% p_z	42	9	47	15	62	30	58	40
total	82	9	88	15	80	30	72	40

[a] Spin properties are averages over the spin density in units of a_0^{-3}. Populations are from an analysis of the CI spin density and refer to valence atomic orbitals (see text).

Table V. Leading Contributions to Properties

		$\langle\delta(M)\rangle$, $\langle 3z^2 - r^2/r^5\rangle_M$, or $\langle 3z^2 - r^2/r^5\rangle_O$			
i	j	BO	CO^+	AlO	SiO^+
		$\langle\delta(M)\rangle$			
ns M	ns M	0.80	1.77	0.85	1.27
$(n-1)$s M	ns M	−0.17	−0.52	−0.65	−0.90
$(n-1)$s M	$(n-1)$s M	0.01	0.04	0.20	0.21
$(n-2)$s M	ns M			0.28	0.36
$(n-2)$s M	$(n-1)$s M			−0.17	−0.17
$(n-2)$s M	$(n-2)$s M			0.03	0.03
p_zO	ns M	0.02	0.06	−0.04	−0.05
p_zO	$(n-1)$s M			0.02	0.02
		$\langle 3z^2 - r^2/r^5\rangle_M$			
np$_z$M	np$_z$M	0.28	0.74	0.41	0.70
$(n-1)$p$_z$M	np$_z$M			0.20	0.31
$(n-1)$p$_z$M	$(n-1)$p$_z$M			0.08	0.08
np$_x$M	np$_x$M	−0.01	−0.05	−0.02	−0.01
np$_y$M	np$_y$M	−0.01	−0.05	−0.02	−0.01
p_zO	np$_z$M	0.04	0.10	0.00	0.01
p_zO	ns M	−0.02	−0.04	−0.02	−0.02
p_zO	p_zO	0.01	0.03	0.03	0.05
		$\langle 3z^2 - r^2/r^5\rangle_O$			
p_zO	p_zO	0.23	0.42	1.36	1.95
p_xO	p_xO	0.08	0.11	0.04	0.01
p_yO	p_yO	0.08	0.11	0.04	0.01
ns M	p_zO	−0.06	−0.11	−0.07	−0.10
np$_z$M	p_zO	0.06	0.12	0.05	0.11
ns M	ns M	0.04	0.08	0.01	0.02
ns M	np$_z$M	−0.05	−0.11	−0.02	−0.03
np$_z$M	np$_z$M	0.05	0.09	0.01	0.02

onto this basis had a trace greater than 0.99, so this minimum atomic basis was adequate for describing the spin density. In this basis, the population of all core orbitals was less than 0.5% so they are not included in Table IV.

In the second method of obtaining spin populations, the theoretical properties were divided by the same free atom parameters used in Table I to convert experimental properties to populations. In spite of the fact that these "experimental" populations still total 100 ± 10%, they are markedly different from the Mulliken gross populations for the same wave function. These numbers do resemble those in Table I, however. In particular, they exhibit the same bothersome trend in the ratio % s/% p noted for the experimental data. The theoretical populations, on the other hand, show the expected trend toward less hybridization in the second row.

In terms of the basis of real atomic orbitals, f_i, the spin density can be written as

$$P = \sum_{ij} P_{ij} f_i f_j$$

If the overlap is $S_{ij} \rightarrow S_{ij} = \langle f_i | f_j \rangle$, then P is normalized so that $1 = \sum P_{ij} S_{ij}$. If the f_i on each center are orthonormal, the Mulliken net population in orbital f_i is p_{ii} and the gross population is

$$n_i = \sum_j p_{ij} \delta_{ji}$$

The diatomic molecules discussed here are fairly ionic, and the net populations of the valence orbitals do not differ qualitatively from the gross populations.

The average value of any property can be written as

$$\theta = \sum_{i>j} t_{ij}$$

where

$$t_{ij} = P_{ij} \langle f_i | \theta | f_j \rangle (2 - \delta_{ij})$$

Table V gives a list of the leading contributions t_{ij} to each property. The experimental analysis is based on the assumption that only one term is important in computing the average. Comparison of Tables IV and V shows that the leading cause of discrepancy between experimental and theoretical populations is the contribution from additional terms involving the core orbitals.

The inner s shells on the metal make large negative contributions to A_{iso}. Similarly, for the second-row metals there is a significant inner-shell contribution to A_{dip} of opposite sign. The result is that A_{iso}/A_{dip} is 1.8 when only the leading term is considered but 0.6 when the whole sum is included. This large change completely invalidates the usual FACM procedure for determining the % s/% p ratio from experimental data. For BO and CO^+ the effect is much less pronounced because they have no inner p core and the 1s core contribution is not as extreme.

At the oxygen end A_{iso} is almost zero. For A_{dip} there are no inner p shells and the net two-center contribution is small. For BO and CO^+, however, there is appreciable spin polarization of the π_i orbital by the σ unpaired electron. This results in a non-negligible negative spin density in the p_x and p_y oxygen orbitals. Because $\langle P_x|(3z^2 - r^2)/r^5|p_x\rangle$ is $-^1/_2$ of $\langle p_z|3z^2 - r^2/r^5|p_z\rangle$, the "experimental" population really measures the anisotropy $p_{zz} - {}^1/_2p_{xx} - {}^1/_2p_{yy}$. This theoretical quantity is in closer agreement with the "experimental" population. Unfortunately, for BO and CO^+, these populations are small so the Mulliken net populations (0.09 for p_z of CO^+) which enter the calculation of the property are appreciably larger than the gross populations (0.06 for p_z of CO^+).

The large inner-shell effect is not due to spin polarization. The singly occupied natural orbital of the leading Slater determinant in the spin-restricted INO expansion gives −789 MHz for A_{iso} (^{29}Si). This effect is best regarded as due to core − other valence overlap. For the wave functions described here, the largest effect comes from the overlap of the p_z orbital of oxygen with the core orbitals of the metal. Because of this overlap, the valence MO containing the unpaired electron has the approximate form

$$c_1(n\text{sm}) - c_2(n\text{pm}) + c_3[(\text{pO}) + S_s((n-1)\text{sm}) + S_p((n-1)\text{pm})...]$$

where $S_s = -\langle \text{pO}|(n-1)\text{sm}\rangle$ and $S_p = -\langle \text{pO}|(n-1)\text{pm}\rangle$. If all p orbitals are positive toward the right and all orbitals are positve at their outer radial maximum, then from Figure 3 we can see that the numerical coefficients (c_1, c_2, c_3, S_s, and S_p) in this MO are positive as it is written.

The inner shells are easily seen to have zero gross population because their net populations are exactly cancelled by their share of the overlap population. Nevertheless, they can make large contributions to operators which are large near the nucleus. This fact has been noted previously in discussions of the extra molecular relativistic correction.[44] Core–other valence overlap has also been shown to be responsible for the weak bond in Na_2.[45] The second largest contribution to A_{iso} in Table V comes from the off-diagonal term

$$2c_1c_3S_s\langle n\text{sm}|\delta(r_m)|(n-1)\text{sm}\rangle$$

which is negative because the ns and $(n-1)$s orbitals have opposite signs at the nucleus. Similarly, the second largest contribution to A_{dip} comes from

$$-2c_2c_3S_p\langle n\text{pm}|(3z^2 - r^2)/r^5|(n-1)\text{pm}\rangle$$

which is positive because the integrand is negative where it is largest.

Conclusion

An experimental procedure for generating and trapping high-temperature radical cations in neon matrices at 4 K for detailed spectroscopic study has been presented. The $^2\Sigma$ radicals $^{28}SiO^+$ and $^{29}SiO^+$ have been examined by ESR and compared with similar results for $^{13}CO^+$ and the isoelectronic AlO radical.

Ab initio CI calculations produced hyperfine properties in good agreement with experiment for the SiO^+ radical cation, but only after the orbitals used in the CI were redefined via MCSCF or INO procedures so as to properly reflect the nature of the unpaired spin density. In the absence of experimental data for this radical there was no indication that low-energy CI wave functions in terms of the original SCF orbitals would be in error by over 560 MHz for $A_{iso}(^{29}Si)$.

Spin populations dervied from experimental data for $^{29}SiO^+$ and AlO by the commonly applied method of comparing molecular A_{iso} and A_{dip} values with similar free atom parameters are significantly different from spin populations derived from wave functions which reproduce the experimentally determined values of A_{iso} and A_{dip}. Such "experimental populations" can therefore be of very limited utility for cases similar to those treated in detail in this report. The "core–other valence overlap" effect has been shown to account for the major difference between the two methods of obtaining spin populations.

Acknowledgment. Support from the National Science Foundation (CHE-8207327) and the Camille and Henry Dreyfus Foundation is gratefully acknowledged (L.B.K.). Part of the theoretical analysis was supported by a grant from the National Science Foundation (ERD).

Registry No. $^{28}SiO^+$, 95616-90-3; $^{29}SiO^+$, 95616-91-4; Ne, 7440-01-9; BO, 12505-77-0; CO^+, 12144-04-6; AlO, 14457-64-8.

(44) Ziegler, T.; Snijders, J. G.; Baerends, E. J. *J. Chem. Phys.* **1981**, *74*, 1271. Pyykkö, P.; Snijders, J. G.; Baerends, E. J. *Chem. Phys. Lett.* **1981**, *83*, 432. Katriel, J.; Feller, D.; Davidson, E. R. *Intl. J. Quantum Chem.*, in press.

(45) Pellissier, M.; Davidson, E. R. *Intl. J. Quantum Chem.*, in press.